ISSN 1063-7826, Semiconductors, 2006, Vol. 40, No. 11, pp. 1304–1313. © Pleiades Publishing, Inc., 2006.
Original Russian Text © A.G. Milekhin, C. Himcinschi, M. Friedrich, K. Hiller, M. Wiemer, T. Gessner, S. Schulze, D.R.T. Zahn, 2006, published in Fizika i Tekhnika Poluprovodnikov, 2006, Vol. 40, No. 11, pp. 1338–1348.

Infrared Spectroscopy of Bonded Silicon Wafers

A. G. Milekhin[a]^, C. Himcinschi[b], M. Friedrich[c], K. Hiller[d], M. Wiemer[d], T. Gessner[d], S. Schulze[c], and D. R. T. Zahn[c]

[a]*Institute of Semiconductor Physics, Siberian Division, Russian Academy of Sciences, Novosibirsk, 630090 Russia*
^e-mail: milekhin@thermo.isp.nsc.ru
[b]*Max-Planck-Institut für Mikrostrukturphysik, D-06120 Halle, Germany*
[c]*Institut für Physik, Technische Universität Chemnitz, D-09107 Chemnitz, Germany*
[d]*Zentrum für Mikrotechnologien, Technische Universität, D-09107 Chemnitz, Germany*

Submitted February 13, 2006; accepted for publication February 27, 2006

Abstract—Infrared spectra of multiple frustrated total internal reflection and transmission for silicon wafers obtained by direct bonding in a wide temperature range (200–1100°C) are studied. Properties of the silicon oxide layer buried at the interface are investigated in relation to the annealing temperature. It is shown that the thickness of the SiO_2 layer increases from 4.5 to 6.0 nm as the annealing temperature is increased. An analysis of the optical-phonon frequencies showed that stresses in the SiO_2 relax as the annealing temperature is increased. A variation in the character of chemical bonds at the interface between silicon wafers bonded at a relatively low temperature (20–400°C) is studied in relation to the chemical treatment of the wafers' surface prior to bonding. Models of the process of low-temperature bonding after various treatments for chemical activation of the surface are suggested.

PACS numbers: 81.20.Vj, 81.65.Cf, 78.30.Am

DOI: 10.1134/S1063782606110108

1. INTRODUCTION

The technology of direct wafer bonding makes it possible to connect two mirror-polished wafers without using any adhesive [1]. To this end, two wafers whose surfaces were preliminarily cleaned of mechanical particles and activated using chemical or plasma-assisted treatment are brought into a close contact with subsequent thermal annealing. The initial bonding (or prebonding) is accomplished at room temperature using a low pressure at the center of the wafers in an ultraclean room in order to keep mechanical particles from coming to the surfaces in contact. The final bonding is attained using a thermal annealing that gives rise to chemical reactions at the interface; these reactions ensure the bonding of the two wafers. This technology is widely used in microelectronics, high-power electronics, micromechanics, and optoelectronics [1–3]. The range of materials that are used for bonding include not only silicon but also III–V compounds, quartz, glass, silicon carbide, sapphire, and a number of other materials. This technology is relatively simple and makes it possible to produce the materials' combinations that are unattainable by other methods. As a rule, high-quality bonding is attained in the case of hydrophilic Si surfaces at high annealing temperatures (above 800°C). At the same time, the technological processes of the devices' production require a decrease in the bonding temperature (to below 400°C) with the high-quality of the bonding retained. Therefore, the main scientific challenge consists in gaining insight into the physical processes that occur at the interface between the two wafers during bonding and, which is particularly important, at relatively low temperatures. This challenge is nontrivial since the range of methods for studying buried heteroboundaries is very limited [1]; infrared (IR) spectroscopy occupies a very important place among these methods. First, IR spectroscopy is a nondestructive and a rapid method and does not require special treatment of the sample. Second, this method features a very high sensitivity to the state of chemical bonds and makes it possible to control the process of chemical reactions and the chemical composition at the interface between the bonded wafers. Third, the use of IR spectroscopy makes it possible to study the structural properties (thickness and stresses) of the nanometer-thick oxide layer that forms at the buried heteroboundary. As shown previously in [1, 4–8], the IR spectroscopy can be used with good results for studying the chemical processes that occur in the course of high-temperature bonding. However, information about the oxide layer [9–12] and data obtained from the IR spectroscopy of silicon wafers bonded at a relatively low temperature (400°C and lower) [8, 13] are rather scarce and contradictory.

In this paper, we report the results of the IR spectroscopy studies of the silicon wafers bonded using various methods of surface activation in a wide range of temperatures. Our primary focus is on two aspects: the study of the oxide-layer properties and the chemical state of the interface between the wafers.

2. EXPERIMENTAL

The IR spectra were recorded using a Bruker IFS 66 IR Fourier spectrometer in the spectral range of 650–4000 cm^{-1} with the resolution of 1 cm^{-1}. In order to study the silicon oxide buried at the interface between silicon wafers, we used the standard method of measuring the IR transmission spectra. These spectra were recorded in the case of oblique incidence at an angle $\theta \approx 70°$ in the p-polarized light (the electric-field vector was parallel to the plane of incidence). This configuration for thin layers (for example, of silicon oxide) makes it possible to study both the transverse (TO) and longitudinal (LO) optical phonons as a result of the Berreman effect [14].

A study of the chemical state of the interface requires another approach. Since the wavelength of IR radiation exceeds the interface-region thickness, absorption at the chemical bonds of the heteroboundary is extremely low. Therefore, the use of the standard method for measuring the IR transmission of the structures is very inefficient. In the situation where the substrate is a transparent material for IR radiation (which is, in particular, the case for silicon in the frequency range of 2000–5000 cm^{-1}, where most of the vibrations at the heterointerface of interest to us are located), the method of multiple frustrated total internal reflection (MFTIR) is used. One of the possible variants of implementation of the MFTIR method includes the fabrication of a prism of a material that has a large refractive index, as is illustrated in Fig. 1a. Infrared radiation enters the sample under the angle θ_{MIT} with respect to its surface, undergoes the frustrated total internal reflection, and exits from the other side face of the prism, thus giving rise to an evanescent wave at the surface. In this case, the intensity of absorption by the buried layer is proportional to the number of passes the IR radiation makes through the prism. This very method makes it possible to study the surface layers with a small refractive index since the evanescent wave penetrates into these layers with exponential attenuation as larger depths are reached (the term "frustrated" reflection has its origin here). However, a serious disadvantage of the configuration under consideration is the necessity of performing mechanical treatment of the sample; this treatment profoundly affects the state of the surface. Mechanical treatment can also bring about a rebonding (separation) of the wafers bonded at comparatively low temperatures. We used another method for measuring the MFTIR spectra [15, 16] based on the use of the MFTIR components made specially of KRS-5 (thallium bromide–iodide, 42% of TIBR/58% of TIJ), as shown in Fig. 1b.

The MFTIR components were polished prisms with an angle of 62° at the base (internal angle of incidence of 38°) in order to attain the optical contact with the surface of the silicon wafer. The radiation enters one of the components, then enters the wafer, undergoes total internal reflection, traverses the interface multiply, and exits from another component. The IR absorption in the buried layer increases appreciably as a result of multiple passes of radiation through the interface. In this case, there is no need for mechanical or chemical treatment of the sample, while the number of passes of the IR radiation through the buried heteroboundary can be easily varied from 30 to 200, depending on the distance between the components.

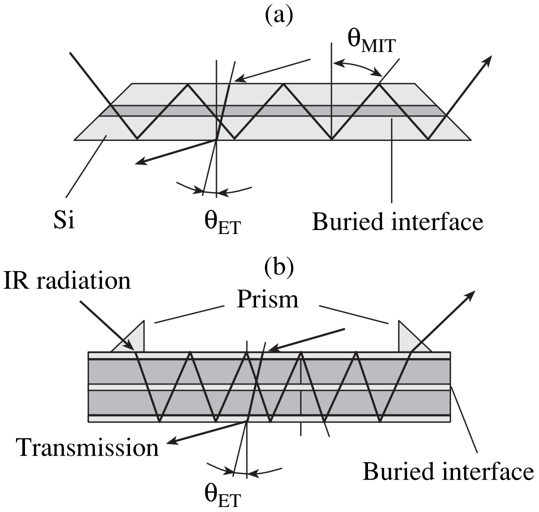

Fig. 1. Layout of the experiment: (a) the MFTIR prism made of the bonded Si wafers and (b) the MFTIR components pressed to the bonded wafers. The geometry of the single-pass transmission in the case of the oblique incidence (angle θ_{ET}) is also illustrated.

In Fig. 2, we show for comparison the IR spectrum of single-pass transmission and the MFTIR spectrum for bonded silicon wafers. It can be seen that the IR spectrum of single-pass transmission yields information about optical phonons in the interfacial oxide layer (absorption at 1000–1200 cm^{-1}), whereas the MFTIR spectrum makes it possible to observe the vibrations of a number of chemical groups at the interface. As has been shown previously [6, 17], the absorption component normal to the surface in the three-layer structure (in the case under consideration, the component normal to the surface of bonded silicon wafers) exceeds multiply the parallel component. In the case of using the MFTIR configuration, the factor of increase in the normal component per single passage equals ~50. If we take into consideration that the number of passes used in the MFTIR configuration is equal to 30–200, we find that the sensitivity of the MFTIR configuration exceeds by two–three orders of magnitude the sensitivity of single-pass transmission to the absorption component perpendicular to the surface. It is for this reason that we used the MFTIR configuration and analyzed the p-polarized IR radiation in order to attain the maximum

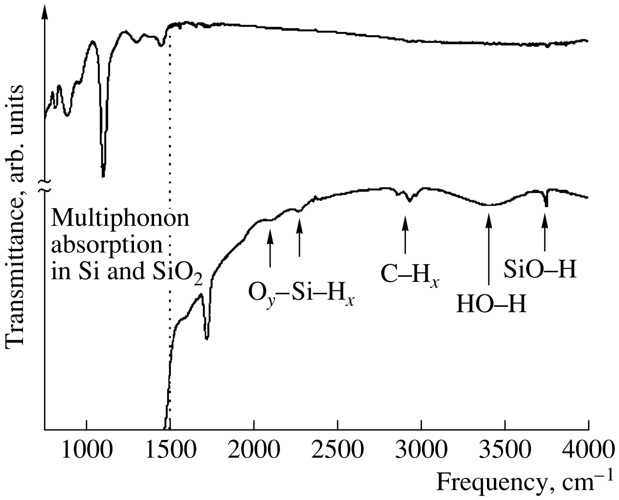

Fig. 2. Infrared spectra of transmission (above) and MFTIR (below) for the bonded Si wafers.

sensitivity. Another reason for using the *p* polarization is the fact that the *p*-polarized light interacts with the bonds that are positioned perpendicularly to the interface; these bonds are involved to the greatest extent in the process of bonding.

3. CHEMICAL TREATMENT OF THE SURFACE OF SILICON WAFERS

For the bonding process, we used *p*-Si (100) wafers grown by the Czochralski method (100 mm in diameter, 463-μm thick, 10–40 Ω cm, polished on both sides). In order to obtain the hydrophilic surfaces of silicon wafers with the aim of attaining the maximum bond force in the course of bonding, we used both chemical treatment and plasma-assisted activation of the surface. The types of preliminary treatments are listed in the table. Samples 1 and 2 were treated in an O_2 plasma but in different reactors (a barrel reactor was used for sample 1, while a reactor for reactive ion etching (RIE) was used in the case of sample 2) with subsequent RCA cleaning of both samples.

The conventional cleaning procedure (RCA) is carried out in an H_2O–H_2O_2–NH_4OH mixture, which ensures the removal of organic compounds due to the solvating effect of ammonium hydroxide and the oxidizing effect of hydrogen peroxide. Cleaning in this solution is carried out for 10–20 min at temperatures of 75–85°C with subsequent cooling of substrates to room temperature, rinsing in deionized (DI) water, and drying in a centrifuge [18]. It is known that, under normal conditions, the surface of single-crystal silicon is coated with a layer of natural oxide with the thickness of ~3 nm; three–four monolayers of water are typically adsorbed on the surface of this oxide. It was found previously [19] that the surface of silicon oxide contains approximately 4.6 of OH groups per 1 nm^2. In addition, two types of silanol (Si–OH) groups exist on the surface: isolated groups and groups connected via hydrogen. The latter groups are formed in the case where the density of isolated groups is high and they are oriented so that the hydrogen bond can be formed.

Prior to bonding, the surface of Si wafers is activated using standard chemical treatment (RCA) based on the following reactions of H^+ or OH^- groups with natural oxide [2]:

$$\begin{aligned}(\text{Si–O–Si}) + \text{OH}^- &\longrightarrow (\text{Si–OH}) + (\text{Si–O}^-),\\ (\text{Si–O}^-) + \text{HOH} &\longrightarrow (\text{Si–OH}) + \text{OH}^-;\end{aligned} \tag{1}$$

$$(\text{Si–O–Si}) + \text{H}^+ + \text{HOH} \longrightarrow (2\text{Si–OH}) + \text{H}^+. \tag{2}$$

The H^+ and OH^- ions control the hydrophilic properties of the surface.

Methods of chemical treatment of the surface of silicon wafers prior to the prebonding process and the corresponding bond energies measured after bonding

Sample no.	Type of treatment	Parameters of subsequent cleaning	Duration, min	Temperature, °C	Bonding energy, J/m^2
1	O_2 plasma, a barrel reactor	p = 1.33 Pa, P = 800 W, RCA cleaning or rinsing in DI water	15		2
2	O_2 plasma, reactive ion etching (RIE) reactor	p = 10 Pa, P = 50 W, U_{bias} = 100 V, RCA cleaning or rinsing in DI water	5		1.26
3	RCA	1) $NH_4OH : H_2O_2 : H_2O = 1 : 1 : 5$ (cleaning)	10	75	1.1
		2) Rinsing in DI water	15	300	
		3) $HCl : H_2O_2 : H_2O = 1 : 1 : 5$	10	75	
		4) Rinsing in DI water	15	300	
		5) $NH_4OH : H_2O_2 = 1 : 1 : 5$	10	75	
		6) Rinsing in DI water	15	300	
4	NH_3 plasma	Rinsing in DI water	15		0.53

Note: p stands for pressure; P, for power; and U_{bias}, for bias voltage.

Equations for reactions (1) and (2) can be rewritten as

$$(\text{Si–O–Si}) + \text{HOH} \longrightarrow (\text{Si–OH}) + (\text{OH–Si}). \quad (3)$$

Equation (3) is valid only in the case where the siloxane bonds are strained [20]. The average angle for the Si–O–Si bond in the natural oxide is equal to ~130°, which differs from the corresponding value (~144°) for the thermal silicon oxide.

The silanol groups are especially important for the bonding process since they can polymerize and form siloxane bridges between the surfaces of two silicon wafers. Treatment in an O_2 plasma in two types of reactors (see table) gives rise to defects on the surface and thus enhances the chemical activity. The methods for activating the surface for bonding at relatively low temperature will be considered below.

The bonding process was controlled using an IR photometry system that made it possible to obtain the IR images of bonded wafers in the transmission mode.

The prebonding was accomplished at a low pressure with the wafers positioned horizontally. A point contact initiates the bonding front that propagates over the wafer for several seconds. The IR image of the samples (recorded after the prebonding procedure) indicated that there are bubbles and other unconnected regions. After the prebonding, the samples were annealed at $T =$ 400–1200°C in nitrogen flow. The IR transmission of the structures was measured again after annealing. The razor method [21] was used to determine the strength of bonding. The error in determination of the bonding energy by this method is ~10%.

4. A MODEL OF HIGH-TEMPERATURE BONDING

Three main stages of the process can be recognized in the model of high-temperature bonding [1, 5–7].

(i) If temperature is below 400°C, the water molecules at the interface react with the thin oxide layer formed as a result of chemical treatment of the surfaces and/or diffuse through this layer, thus forming an additional oxide layer at the Si/SiO_2 heteroboundary; i.e., we have

$$H_2O \longrightarrow Si/SiO_2 + 2(O_x)SiH \quad (4)$$

or

$$Si + 2H_2O \longrightarrow SiO_2 + 2H_2.$$

(ii) If temperatures exceed 400°C, Si–O–Si bonds are formed as a result of decomposition of the hydroxyl groups (OH) at the heteroboundary. It is assumed that the mechanism in this stage consists of the reaction of the surface silanol groups with resulting release of hydrogen:

$$(\text{–Si–OH}) + (\text{–Si–OH}) \longrightarrow (\text{–Si–O–Si–}) + H_2, \quad (5)$$

where the –Si–O–Si– bonds form bridges between the oxidized surfaces of the two wafers. Thus, local areas of bonded wafers are formed.

(iii) Starting with temperatures of 800°C and higher, a drastic increase in the bonding strength for the two wafers occurs. At these temperatures, the SiO_2 viscosity at the heteroboundary decreases appreciably, which increases the contact area and gives rise to additional siloxane bonds. The fate of the H_2 molecules formed as a result of dissociation of water molecules is, strictly speaking, unknown. It is assumed that some H_2 molecules diffuse from the region under consideration into the Si crystal, while some of them are concentrated at the interface and form bubbles.

5. DETERMINATION OF PROPERTIES OF THE BURIED OXIDE LAYER

Variations in the thickness and structure of the buried silicon oxide layer as a result of heat treatment at various temperatures were studied by analyzing the IR spectra in the region of the SiO_2 reststrahlen band (Fig. 3a). Two features are observed in the IR spectra; one feature is located at 1107 cm^{-1} and the other in the vicinity of 1250 cm^{-1}. The absorption band near 1250 cm^{-1} is caused by the LO phonons; its position and intensity vary. The shift of the frequency of LO phonons (from 1247 to 1256.5 cm^{-1}) for connected Si wafers after prebonding and after a high-temperature annealing will be discussed below. The intense line at 1107 cm^{-1} corresponds to the absorption by interstitial oxygen in crystalline silicon; only a poorly pronounced shoulder near 1050 cm^{-1} is related to absorption by the TO vibrations in silicon oxide. The inset in Fig. 3a shows that absorption at 1107 cm^{-1} decreases by 0.5% as a result of annealing. This means that interstitial oxygen diffuses from bulk silicon towards the surface and buried interface with subsequent formation of silicon oxide [9].

The IR transmission spectra of bonded silicon wafers contain information about both the surface and interfacial layers of silicon oxide. In order to discriminate between the contributions made by these two layers to the IR spectra, we removed the oxide layer at the surface of bonded wafers in the course of chemical etching in an HF solution (40%). The IR spectra of bonded layers after etching were measured in the same configuration; these spectra are shown in Fig. 3a by dashed lines. As can be seen from Fig. 3a, the position of the LO-phonon band remained practically unchanged after etching. This behavior implies that the structure of the oxide at the surface is close to that of the oxide at the buried interface. In addition to the fact that the frequency of LO phonons in SiO_2 remains unchanged after etching, the intensity of these modes and the shoulder at 1050 cm^{-1} decrease appreciably as a result of etching.

In order to obtain a response from the layer of surface oxide, the IR spectra of as-prepared bonded wafers (the solid lines in Fig. 3a) were normalized to the spectra of the samples subjected to chemical etching (dashed curves in Fig. 3a). The T_n/T_e spectra obtained as

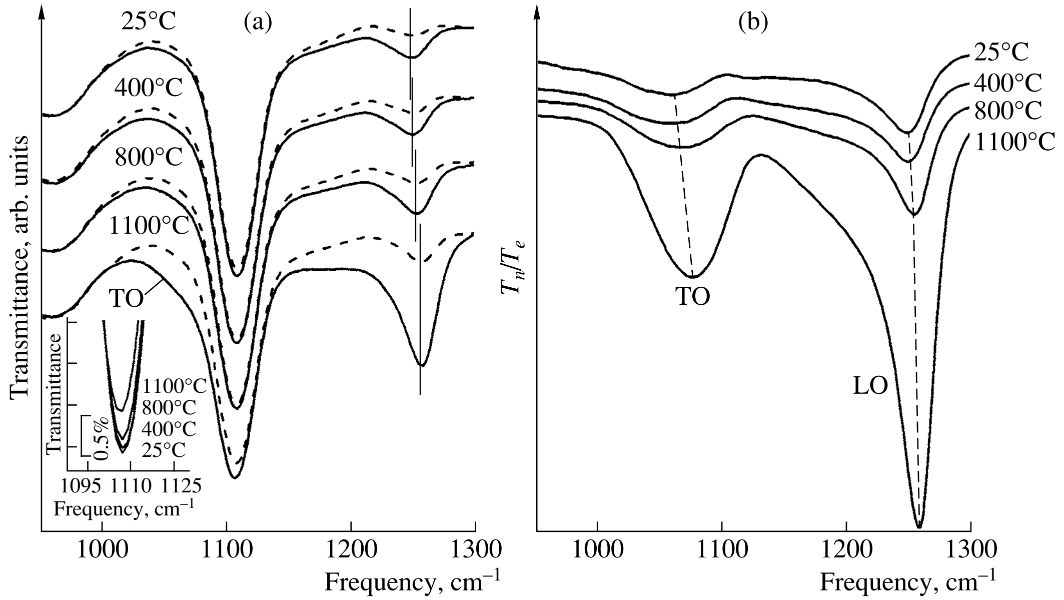

Fig. 3. (a) Infrared transmission spectra of bonded Si wafers after annealing at different temperatures without (solid lines) and after (dashed lines) etching of the surface; the inset illustrates the comparison of transmittance in the band at 1107 cm^{-1}. (b) Normalized spectra related to absorption in silicon oxide on the surface of bonded silicon wafers.

a result of this normalization are shown in Fig. 3b. This procedure makes it possible to reveal the absorption lines related to the TO phonons and located in the vicinity of 1050 cm^{-1}. An increase in the intensity of the bands related to the LO and TO phonons as a result of annealing is accounted for by an increase in the thickness of the surface-oxide layer, which is confirmed by the ellipsometry data [12]. As the annealing temperature increases, the frequency of both vibrational modes shift to higher frequencies; however, the shifts of the TO and LO modes are different.

Evidently, the frequencies of TO and LO modes increase as the annealing temperature is increased; it is noteworthy that the shift of the TO-phonon frequency is larger. This circumstance brings about a decrease in the LO–TO splitting. There are two possible causes of this variation: relaxation of stresses in the layer of silicon oxide, and a change in the stoichiometry of this oxide. However, as shown by Queeney et al. [22], an improvement in the stoichiometry at the Si/SiO$_2$ interface as the thickness of the oxide layer increases (i.e., as the content of SiO$_2$ in the SiO/SiO$_2$ mixture increases) is accompanied by an increase in the LO–TO splitting. Therefore, the observed decrease in the magnitude of expansion as the annealing temperature is increased cannot be accounted for by an improvement of the stoichiometry. Consequently, the relaxation of stresses can be responsible for the observed behavior of the TO and LO phonons.

The central-force network model for the lattice [23, 24] yields a relation between the frequencies of the LO and TO phonons and either stresses in the surface oxide layer or the angle of the Si–O–Si bridge bond [25]. Using experimental values for the frequencies of TO phonons, we find that the angle of the Si–O–Si bond increases from 137.7° for silicon wafers after prebonding to 143° for the structures annealed at 1100°C. Thus, an increase in the annealing temperature brings about an increase in the TO-phonon frequency, which is consistent with an increase in the angle of the Si–O–Si bond. The variation in the frequency of optical phonons as a result of annealing as observed in the IR experiments is more likely consistent with the behavior of phonons in vitreous SiO$_2$ [26] rather than in chemically produced [27] or thermally grown [26] silicon oxide.

The frequency positions of the bands related to LO phonons in silicon oxide in bonded silicon wafers before and after etching coincide with each other according to the IR experiments. If the magnitude of the LO–TO splitting is also not changed as a result of etching, it is most likely that the structure of the surface and interface oxides remains unchanged.

The thickness of the surface silicon oxide layer can be determined with a high accuracy using ellipsometry, whereas the characterization of the interfacial oxide layer is impossible as a result of the small depth of penetration of light into silicon in the visible and ultraviolet spectral regions. Therefore, the thickness of the buried silicon oxide layer in the bonded silicon wafers was determined using IR spectroscopy [12]. In order to determine the oxide-layer thickness, we fit the IR transmission spectra calculated using the method of *E–H* matrices for multilayer structures [28] to the experimental spectra of bonded structures. The surface oxide layer of these wafers was removed preliminarily.

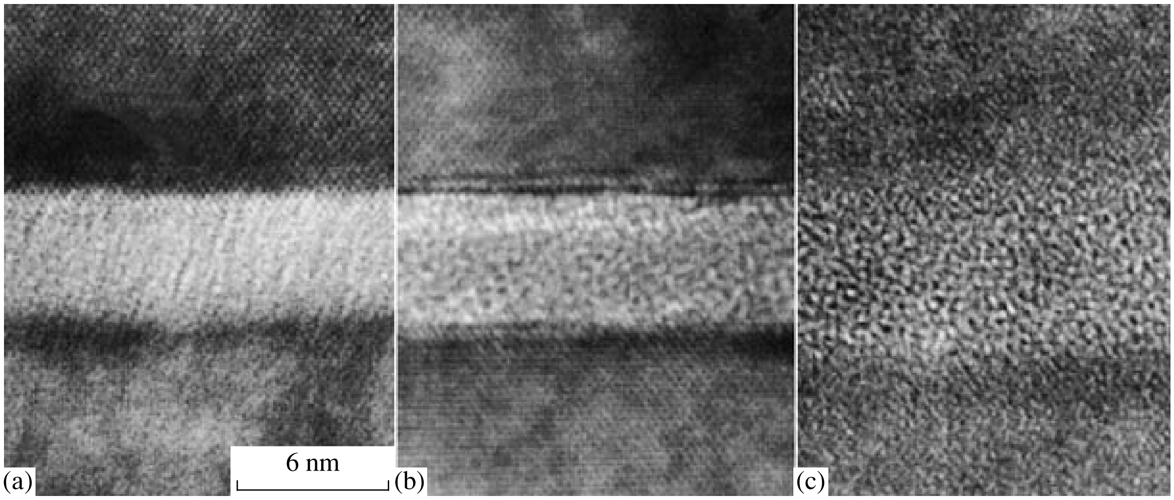

Fig. 4. The HREM images of a transverse section in the interfacial region of the bonded silicon wafers annealed at temperatures of (a) 400, (b) 800, and (c) 1100°C.

The extinction coefficient for silicon is highly sensitive to variation in the concentration of interstitial oxygen in bulk silicon (the absorption band at 1107 cm^{-1}). Therefore, the value of this coefficient was obtained from the best agreement between the calculated and experimental IR transmission spectra for a single Si wafer whose natural oxide was also etched off preliminarily. Thus, the phonon-related absorption in bulk silicon was taken into account automatically. The obtained extinction coefficient for Si and the published data for silicon oxide [29] were used to calculate the IR transmission spectra for bonded silicon wafers; the thickness of the interfacial oxide layer was an adjustable parameter in the calculations.

The interfacial layer was considered as a SiO_2 layer confined by thin (0.7 nm) mixed SiO_2/SiO layers where the SiO_2 content was 40%. The introduction of a SiO sublayer makes it possible to take into account the nonstoichiometric composition of the interfacial oxide layer [22]. The thickness of the buried layer increases from 4.8 nm for the wafers bonded at room temperature to 5.1, 5.5, and 6.0 nm as a result of subsequent annealing at 400, 800, and 1100°C, respectively. The error in the calculation of the thickness is estimated at 0.25 nm.

In order to verify the obtained results, we additionally measured the interfacial-layer thickness using high-resolution electron microscopy (HREM) [11]. Images of transverse section of the bonded wafers are shown in Fig. 4. It is evident that the results obtained using IR spectroscopy are in good agreement with the HREM data. It is worth noting that the use of the HREM method for characterization of the wafers after prebonding was unavailable as a result of the low bonding energy of the wafers, which resulted in their separation in the course of preparation of the samples for experiments with HREM.

6. CHEMICAL STATE OF THE BURIED HETEROBOUNDARY: A HIGH-TEMPERATURE BONDING

In order to gain insight into the mechanism of formation of the interfacial layer, one should not only determine the layer's thickness and internal structure but also identify the chemical states at the interface between the wafers. In Fig. 5, we show the typical IR MFTIR spectra of bonded wafers annealed at different temperatures; the spectra were measured in the spectral region where the absorption lines related to OH and Si–H are observed. As can be seen from Fig. 5a, the IR spectrum of the sample after prebonding features an absorption line at 2105 cm^{-1} caused by stretching vibrations of Si–H in dihydride groups at the Si (100) surface [30]. A broad absorption band centered in the vicinity of 3460 cm^{-1} is related to the stretching vibrations of O–H groups in water molecules adsorbed on the surface of the wafers after prebonding (Fig. 5b). Heat treatment of the structures at 400°C brings about a drastic decrease in the intensity of the band at 3460 cm^{-1} as a result of dissociation of water molecules at the buried interface. In addition, new features appear at 3737 and 3680 cm^{-1}; these features are caused by absorption at stretching vibrations of O–H in silanol groups (Si–OH) isolated and connected, respectively, by the hydrogen bond [4]. Dissociation of water molecules leads to an increase in absorption caused by the stretching vibrations of Si–H at 2105 cm^{-1}. At the same time, a new band centered at 2270 cm^{-1} appears; this band corresponds to absorption by vibrations of Si–H in the O_3–Si–H groups. Subsequent annealing of the samples at 800°C brings about the disappearance of absorption by silanol groups. This fact is accompanied by a decrease in the intensity of the Si–H absorption line at 2105 cm^{-1} and by an increase in absorption by the O_3–Si–H groups at 2270 cm^{-1}. The band related to O_3–Si–H shifts to higher frequencies as

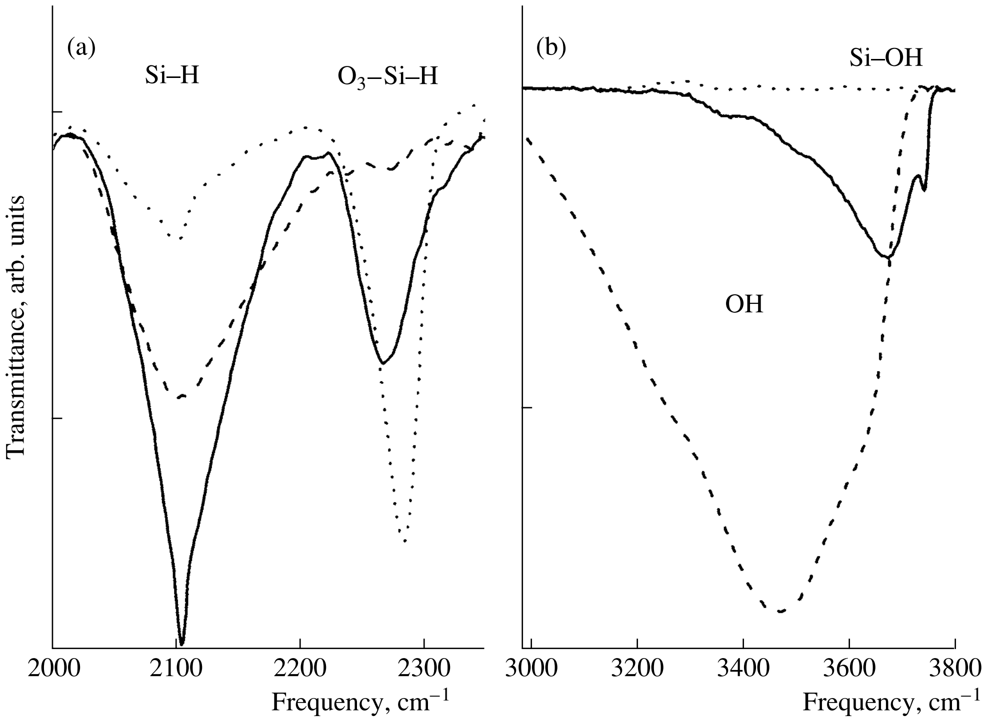

Fig. 5. Infrared MFTIR spectra of bonded Si wafers after prebonding (dashed line) and after subsequent annealing at temperatures of 400°C (the solid line) and 800°C (dotted line). The frequency ranges correspond to vibrations of the (a) Si–H and O_3–Si–H groups and (b) OH and Si–OH groups. The spectra are normalized to the MFTIR spectrum of the structure annealed at 1100°C.

the annealing temperature is increased from 400 to 800°C. This shift is caused by diffusion of hydrogen atoms located at the buried boundary into the bulk of the oxide layer [15].

The obtained experimental data make it possible to evaluate the effect of chemical states on the formation of the interfacial oxide layer as the annealing temperature is increased. At temperatures below 400°C, dissociation of water molecules brings about an increase in the thickness of the buried interfacial layer due to oxidation of crystalline silicon. A further increase in the annealing temperature gives rise to silanol groups that, in turn, are conducive to an increase in the thickness of the oxide layer. These inferences are consistent with the model of bonding suggested in [1, 5–7]. Growth of silicon oxide at the last stage of annealing (800–1100°C) is caused by diffusion of oxygen from bulk silicon into the interfacial region. This mechanism is confirmed by a decrease in the intensity of absorption by interstitial oxygen at 1107 cm^{-1} as the bonding temperature is increased (see the inset in Fig. 3a).

7. A MODEL OF LOW-TEMPERATURE BONDING

In order to obtain the hydrophilic surface of the wafers, we used various chemical and plasma-assisted chemical (in the O_2- and NH_3 plasmas) methods of activation listed in the table. After the prebonding, the samples were annealed at a temperature of 400°C in the nitrogen atmosphere for 6 h. The IR MFTIR spectra were measured before and after the annealing.

Changes in the IR MFTIR spectra of the samples activated by different methods, after prebonding and subsequent annealing, are illustrated in Fig. 6. The samples subjected to prebonding contain water molecules at the interface; these molecules absorb in the spectral region of 3000–3600 cm^{-1} (Fig. 6a) and at 1630 cm^{-1} (this band is caused by bending vibrations and is not shown in Fig. 6). The surfaces of silicon wafers at the interface are partly oxidized and passivated with hydrogen. This circumstance gives rise to absorption at the frequencies of 2105 and 2270 cm^{-1} (Fig. 6b), which corresponds to the stretching vibrations of the Si–H_2 and Si–H bonds in the O_2–Si–H_2 and O_3–Si–H groups in silicon dioxide [31, 32].

The annealing initiates dramatic changes in the chemical states at the interface, so that new chemical bonds are formed, which is confirmed by the data of IR spectroscopy. The drastic decrease in the absolute value of absorption at 3000–3600 cm^{-1} (Fig. 6a) is indicative of dissociation of water molecules adsorbed at the interface. The decrease in the amount of water was evaluated on the basis of calculations [33] from an analysis of absorption by vibrations of the O–H groups; it corresponds to a loss of 1.76 and 3 monolayers of water for samples 1 and 2 (treated in O_2 plasma), respectively, and 1.56 monolayers for sample 3 (RCA treatment). The integrated absorption was calculated in the spectral

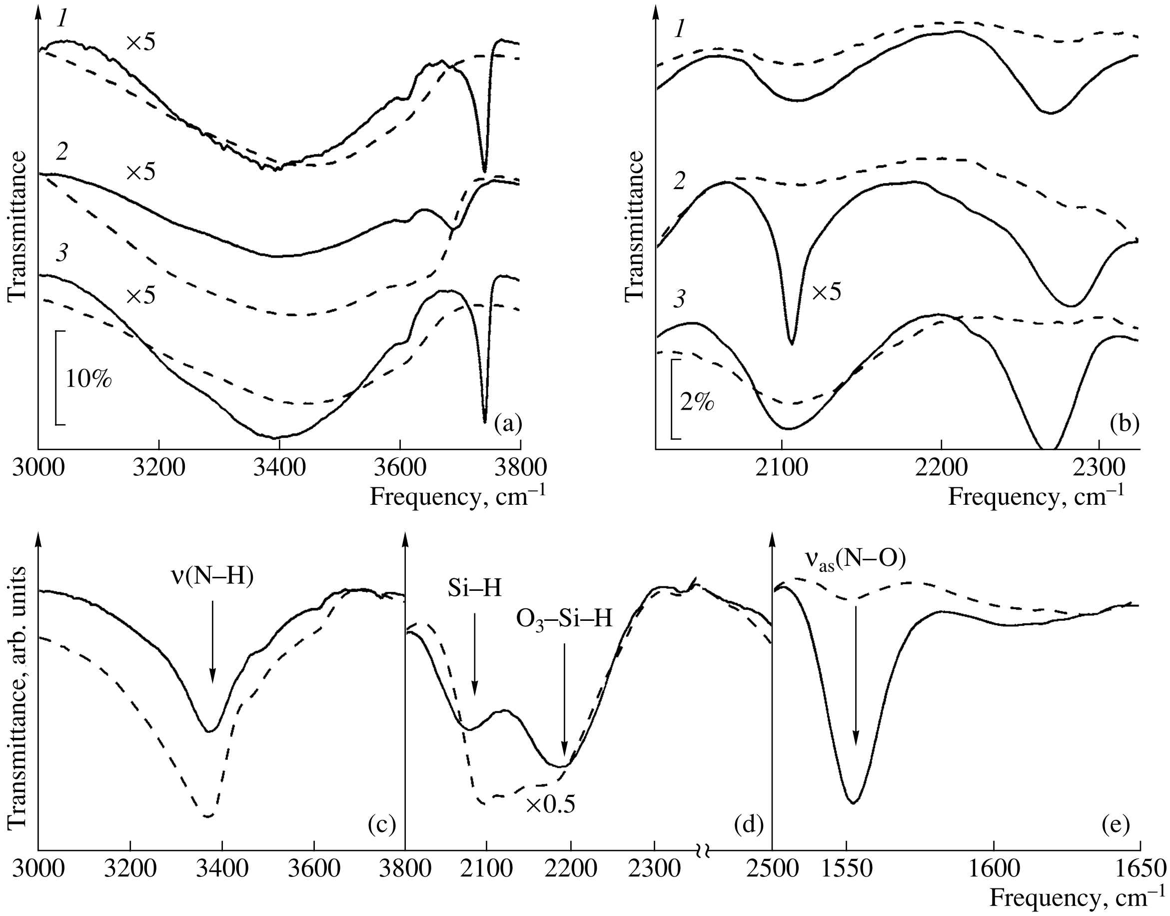

Fig. 6. Infrared MFTIR spectra of bonded Si wafers activated in O_2 plasma (samples 1 and 2, spectra *1* and *2*), by chemical method (sample 3, spectra *3*) (the spectra were measured in the frequency ranges that correspond to vibrations of the (a) O–H and (b) Si–H groups), and activated in NH_3 plasma (samples 4; panels c, d, e). Dashed lines represent the spectra after prebonding, while solid lines correspond to the spectra measured after subsequent annealing at 400°C.

range from 3000 to 3800 cm^{-1}. Dissociation of water molecules causes an increase in the absorption at 2105 cm^{-1} and gives rise to a new line peaked at 3739 cm^{-1} and related to the vibrations of isolated silanol groups at the buried heteroboundary [7]. The concentration of Si–H groups after annealing was calculated using the data obtained from the IR spectra; this concentration amounts to 0.14, 0.19, and 0.23 monolayers for the samples treated in an O_2 plasma (sample 1), subjected to the RCA treatment (sample 3), and treated in an RIE reactor (sample 2), respectively. In this case, the integrated absorption was calculated in the frequency range from 2060 to 2200 cm^{-1}.

The Si–H bond energy is relatively high; as a result, the bonds are rather insensitive to the chemical reactions occurring at the surface [34]. This circumstance retards the formation of the Si–O–Si bridges, which results in a decrease in the bonding energy of the wafers in contact. Oxygen molecules also are not involved in the bonding process since they predominantly attack the Si–Si bonds in the near-surface layer. Indeed, the IR spectra of the Si–Si bonded wafers (treated in an O_2 plasma, sample 1) exhibit a comparatively low absorption at 3739 cm^{-1} (Fig. 6a) and 2105 cm^{-1} (Fig. 6b) and a high bonding energy, >2 J/m^2 (see table). At the same time, in the case of wafers activated using RCA treatment, intense absorption lines are observed in the IR spectra at the same frequencies; however, the bonding energy is now much lower (1.1 J/m^2).

Using this line of reasoning, we might expect that sample 2 should have a higher bonding energy, since the IR spectra are indicative of either very low absorption by silanol groups (Fig. 6b) or its absence. Moreover, the IR spectra of this sample feature a new line peaking at 3685 cm^{-1} and caused by Si–O–H groups in the interfacial SiO_2 layer. This circumstance indicates that an interfacial layer with the thickness of several nanometers is formed, which should bring about an increase in the energy of bonding.

However, as can be seen from the table, the bonding energy of this sample is even lower (1.26 J/m^2) than that of sample 1 treated in O_2 plasma. This means that there must be an additional mechanism that was not taken

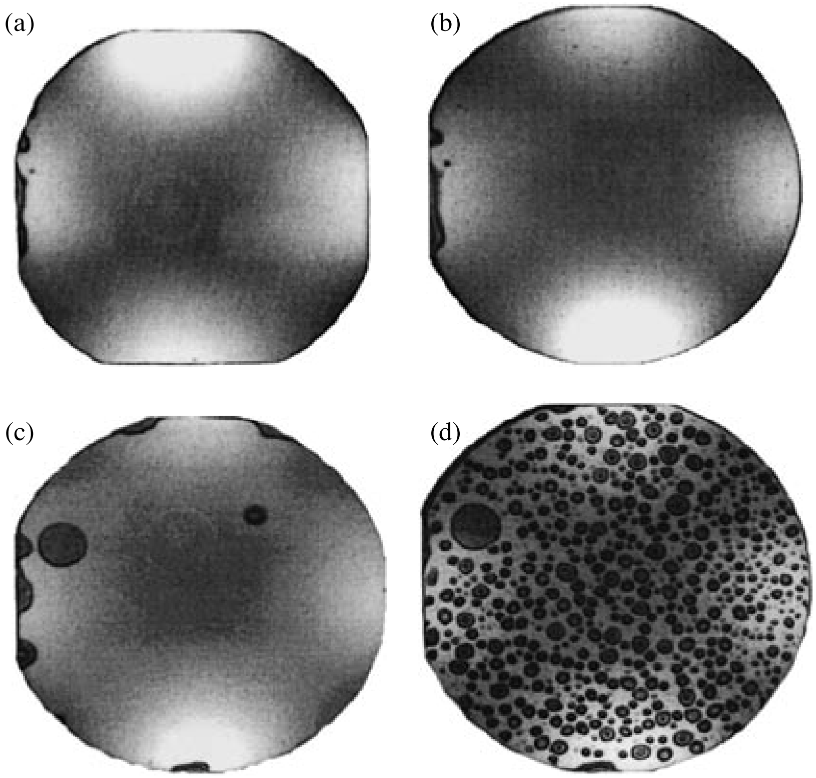

Fig. 7. Infrared images (obtained in the transmission mode) of bonded Si wafers after (a, c) prebonding and (b, d) bonding at 400°C. Preliminary treatment was carried out in (a, b) O_2 and (c, d) NH_3 plasma.

into account in the previous consideration. As follows from the IR data, formation of unconnected regions (bubbles) can be a cause of a decrease in the energy of bonding. Indeed, the IR spectrum of sample 2 includes an intense absorption line at 2105 cm^{-1} (Fig. 6b); this line overlaps with a broad band centered at the same frequency and related to stretching Si–H vibrations at the (100) surface. The narrow absorption line is caused by local vibrations of the Si–H groups at the steps or terraces in unconnected regions of bonded wafers [17]. Dissociation of water molecules is accompanied by a release of a high hydrogen concentration that exceeds the solubility limit for hydrogen in the interfacial region. This circumstance gives rise to a large number of bubbles localized in the interfacial region, which is confirmed by the results of IR photometry. The hydrogen molecules diffuse into the interfacial silicon oxide with resulting formation of O_3–Si–H groups responsible for absorption at 2270 cm^{-1} (Fig. 6b).

The cause of the appearance of the low-intensity absorption line peaked at 3611 cm^{-1} and observed in the IR spectra (Fig. 6a) is unclear. The frequency of this line is close to that (3618 cm^{-1}) of the absorption line observed at 10 K in the IR spectra of silicon wafers after annealing in the H_2 atmosphere and attributed to absorption by the H_2 molecules trapped by impurities or crystal-lattice defects [35]. Such diffusion of hydrogen can also take place in the bonded wafers. However, detailed investigations are needed for unambiguous identification of this line; these investigations are beyond the scope of this study.

Activation of the surface by NH_3 plasma prior to prebonding results in the lowest bonding energy (see table). IR spectroscopy makes it possible to determine the causes of the low bonding energy and identify the bonding mechanism for these structures.

The IR spectra of sample 4 measured after prebonding and subsequent annealing (Figs. 6c, 6d, 6e) include three intense lines at 3370 cm^{-1} (Fig. 6c), 2185, and 2090 cm^{-1} (Fig. 6d), and a weak line at 1550 cm^{-1} (Fig. 6e). The line at 3370 cm^{-1} is caused by absorption at asymmetric stretching vibrations ν of N–H in the NH_2 groups [36]. It cannot be ruled out that this line also overlaps with the broad absorption line for OH groups in water molecules. The lines at 2185 and 2090 cm^{-1} are related to the stretching vibrations of Si–H in the O_2–Si–H group [37] and in the monohydride [31], respectively. The absorption line at 1552 cm^{-1} is related to the asymmetric stretching vibration ν_{as} (N–O) in molecules of nitrogen dioxide NO_2 [36].

Subsequent annealing at T = 400°C brings about appreciable changes in the IR spectra. Absorption by the N–H, O_2–Si–H, and Si–H vibrations is reduced, whereas the intensity of the absorption line related to NO_2 increases drastically. This behavior of the IR spectra can be interpreted in the following way. Activation using treatment in NH_3 plasma gives rise to Si–N–H_2 groups at the surface. In addition, the surface of the wafers is partially oxidized and passivated with hydrogen. This inference is confirmed by the presence of absorption lines related to O_2–Si–H and Si–H groups in the IR spectra. Partial oxidation of the Si–N–H_2 groups with resulting formation of NO_2 molecules even at room temperature is responsible for absorption at 1550 cm^{-1}. It should be noted that the number of water molecules adsorbed at the surface of the wafers is much smaller than in the case of other methods of surface treatment. This statement is validated by low absorption by the scissor vibrations of the OH groups at 1630 cm^{-1}. Dissociation of the O_2–Si–H and Si–N–H_2 groups and formation of Si–O–Si bonds and gaseous products (hydrogen and NO_2) occur in the course of annealing. The evidence for the presence of the NO_2 molecules was obtained from an analysis of the IR spectra related to isolated Si wafers and measured prior to the bonding process. Absorption at 1550 cm^{-1} was not observed in the IR spectra of these structures since gaseous NO_2 is not bound to the Si surface. These gases form a large number of bubbles that can be observed in the IR images of bonded wafers as shown in Fig. 7. Thus, the formation of bubbles results in a decrease in the bonding energy of bonded wafers.

8. CONCLUSIONS

As shown in this study, IR spectroscopy is an efficient nondestructive tool for rapid control of the state of buried heteroboundaries in silicon structures obtained by the method of direct bonding. An analysis of the IR transmission and MFTIR spectra made it possible to describe the properties of the interfacial oxide layer, identify the nature of chemical states at the interface, describe their evolution in the course of annealing, and establish the possible mechanisms of low-temperature bonding.

ACKNOWLEDGMENTS

We are grateful to L.L. Sveshnikova for her careful reading of the manuscript and valuable comments.

REFERENCES

1. Q.-Y. Tong and U. Gösele, *Semiconductor Wafer Bonding: Science and Technology* (Electrochemical Society, New York, 1999).
2. Q.-Y. Tong, W. J. Kim, T.-H. Lee, and U. Gösele, Electrochem. Solid-State Lett. **1**, 52 (1998).
3. K. Hiller, M. Wiemer, C. Kaufmann, et al., in *Proceedings of 10th International Conference on Solid-State Sensors and Actuators, Transducers'99* (Sendai, 1999), p. 1448.
4. D. Feijoo, Y. J. Chabal, and S. B. Christman, Appl. Phys. Lett. **65**, 2548 (1994).
5. R. Stengl, T. Tan, and U. Goesele, Jpn. J. Appl. Phys. **28**, 1735 (1989).
6. M. K. Weldon, Y. J. Chabal, D. R. Hamann, et al., J. Vac. Sci. Technol. B **14**, 3095 (1996).
7. M. K. Weldon, V. E. Marsico, Y. J. Chabal, et al., Surf. Sci. **368**, 163 (1996).
8. Y. J. Chabal, D. Feijoo, S. B. Christman, and C. A. Goodwin, Proc.–Electrochem. Soc. **7**, 305 (1995).
9. K.-Y. Ahn, R. Stegl, T. Y. Tan, et al., Appl. Phys. A **50**, 85 (1990).
10. L. Ling and F. Shimura, J. Appl. Phys. **71**, 1237 (1992).
11. C. Himcinschi, A. Milekhin, M. Friedrich, et al., J. Appl. Phys. **89**, 1992 (2001).
12. C. Himcinschi, A. Milekhin, M. Friedrich, et al., Appl. Surf. Sci. **175–176**, 715 (2001).
13. C. Maleville, O. Rayssac, H. Moriceau, et al., Proc.–Electrochem. Soc. **36**, 46 (1997).
14. D. W. Berreman, Phys. Rev. **130**, 2193 (1963).
15. A. Milekhin, M. Friedrich, K. Hiller, et al., J. Vac. Sci. Technol. B **17**, 1733 (1999).
16. A. Milekhin, M. Friedrich, K. Hiller, et al., J. Vac. Sci. Technol. B **18**, 1392 (2000).
17. Y. J. Chabal, Surf. Sci. Rep. **8** (5–7), 211 (1988).
18. W. Kern and D. A. Puotinen, RCA Rev. **31**, 187 (1970).
19. C. G. Armistead, A. J. Tyler, F. H. Hambleton, and J. A. Hockey, J. Phys. Chem. **73**, 3947 (1969).
20. T. A. Michlske and B. C. Bunker, J. Appl. Phys. **56**, 2686 (1984).
21. W. P. Maszara, G. Goetz, A. Gaviglia, and J. B. McKitterick, J. Appl. Phys. **64**, 4943 (1988).
22. K. T. Queeney, M. K. Weldon, J. P. Chang, et al., J. Appl. Phys. **87**, 1322 (2000).
23. P. N. Sen and M. F. Thorpe, Phys. Rev. B **15**, 4030 (1977).
24. F. L. Galeener, Phys. Rev. B **19**, 4292 (1979).
25. C. Martinet, R. A. B. Devine, and M. Brunel, J. Appl. Phys. **81**, 6996 (1997).
26. K. Ishikawa, U. Uchiyama, H. Ogawa, and S. Fujimura, Appl. Surf. Sci. **117–118**, 212 (1997).
27. A. B. Gurevich, M. K. Weldon, Y. J. Chabal, et al., Appl. Phys. Lett. **74**, 1257 (1999).
28. R. M. A. Azzam and N. M. Bashara, *Ellipsometry and Polarized Light* (North-Holland, Amsterdam, 1977; Mir, Moscow, 1981).
29. *Handbook of Optical Constants of Solids*, Ed. by E. D. Palik (Academic, New York, 1985).
30. Y. J. Chabal, Surf. Sci. **168**, 594 (1986).
31. P. Dumas, Y. J. Chabal, and P. Jakob, Surf. Sci. **269–270**, 867 (1992).
32. H. Ogawa and T. Hattori, Appl. Phys. Lett. **61**, 577 (1992).
33. Z. H. Zhou, E. S. Aydil, R. A. Gottscho, et al., J. Electrochem. Soc. **140**, 1316 (1993).
34. M. Niwano, J. Kageyama, K. Kurita, et al., J. Appl. Phys. **76**, 2157 (1994).
35. R. E. Pritchard, M. J. Ashwin, J. H. Tucker, et al., Phys. Rev. B **56**, 13118 (1997).
36. D. Lin-Vien, N. B. Colthup, W. G. Fateley, and J. G. Grasselli, *The Handbook of Infrared and Raman Characteristic Frequencies of Organic Molecules* (Academic, Boston, 1991).
37. J. A. Schaefer, D. Frankel, F. Stucki, et al., Surf. Sci. **139**, L209 (1984).

Translated by A. Spitsyn